REPRINTED FROM
HIGH-PRESSURE RESEARCH
Applications in Geophysics

ACADEMIC PRESS, INC.
NEW YORK SAN FRANCISCO LONDON

TRANSDUCER AND BOND PHASE SHIFTS IN ULTRASONICS, AND THEIR EFFECTS ON MEASURED PRESSURE DERIVATIVES OF ELASTIC MODULI

G. F. DAVIES
Department of Geological Sciences
University of Rochester
Rochester, New York 14627

R. J. O'CONNELL
Department of Geological Sciences
Harvard University
Cambridge, Massachusetts 02138

Abstract

Phase shifts introduced into ultrasonic signals by the presence of transducers and bonds at sample surfaces have been measured using an automated variable frequency ultrasonic interferometer. At zero pressure, phase shifts have been resolved due to transducers, bonds between transducers and samples, and bonds between buffer rods and samples. Observed transducer-bond-sample phase shifts are in good accord with theoretical estimates, and bond thicknesses of about 0.3 μ are inferred. Measurements to 7 kbar are consistent with theoretical estimates of the effect of pressure on transducer-bond-phase shifts. Providing the frequency of the ultrasonic signal is within a few percent of the resonance frequency of the transducer, and the effect of pressure on the transducer resonance frequency is accounted for (as recommended by *McSkimin*, [1961]), the effect of the bond phase shift on the measured pressure derivative of the elastic modulus should amount to less than about 0.02. If the frequency deviates substantially from the transducer resonance frequency, especially at zero pressure, errors of the order of 0.25 could be incurred in the pressure derivatives. The nonlinearity of transducer-bond phase shifts could cause significant errors in second-pressure derivatives, even under favorable conditions. For shear waves at zero pressure, the observed buffer-bond-sample phase shifts are consistent with those estimated theoretically for a bond of about 1 μ thickness. For compressional waves at zero pressure, phase shifts are very sensitive to the buffer-sample contact: large differences in phase are observed between dry lapped, "wetted," immersed, and resin-bonded contacts. The sources of these differences are not fully understood, but they may be due to variations in contact area produced by the ultrasonic wave. "Normal" buffer-sample bonds are estimated to be capable of affecting measured pressure derivatives by about 0.25. The behavior of the anomalous

buffer-sample phase shifts under pressure is unknown, but the shifts could easily give rise to substantial errors in measured pressure derivatives.

I. INTRODUCTION

The geophysical objective of ultrasonic measurements is to be able to extrapolate laboratory measurements of elastic properties and density to the pressure and temperature conditions of the earth's deep interior. For these extrapolations to be useful, considerable accuracy is required of the measurements. In principle, the widely used pulsed ultrasonic techniques [*McSkimin*, 1957; 1961], or variations thereof, are capable of measuring elastic velocities to an accuracy of at least 0.05%, and of detecting relative changes in elastic velocity of even smaller magnitude [*McSkimin*, 1956]. In practice, however, this accuracy apparently has not usually been achieved.

Table 1 compares the results of different measurements of the same material for several materials: the spread in results for elastic moduli is commonly in the range 0.2-1%, and greater in some cases. The velocity measurements taken to pressures of the order of 10 kbar would show changes of the order of a few percent. Thus, in principle, the measured pressure derivatives of elastic modulus should be accurate to a few percent at least. It can be seen in Table 1, however, that discrepancies of the order of 10% commonly occur. For materials of geophysical interest, an uncertainty of this magnitude produces an uncertainty of the order of 10% in elastic velocities extrapolated to 1 Mbar, and this uncertainty is much too large for the extrapolation to be useful in interpreting the seismically observed elastic velocities in the deep mantle. It is thus of interest to determine the source of the discrepancies.

This paper reports on the effects of phase shifts in ultrasonic waves caused by the presence of transducers, buffer rods, and bonding material at the surface of a sample. These phase shifts are one possible source of the discrepancies discussed above. Theoretical and experimental determination of buffer-bond phase shifts at zero pressure were considered by *McSkimin* [1950; 1957]. Transducer-bond phase shifts were considered by *Redwood and Lamb* [1956] and *McSkimin* [1957; 1961]; the effects of pressure and temperature were considered by *McSkimin* [1961] and *McSkimin and Andreatch* [1962]. In this study the phase shifts were observed over a wide frequency range using ultrasonic interferometry, and the effects of pressure are considered in more detail.

TABLE 1. Comparison of Different Measurements of Elastic Moduli and Their Pressure Derivatives (Denoted by a Prime) for Several Materials[a]

Material	*Elastic Moduli*, Mbar				*Pressure Derivatives*				Reference
	C_{11}	C_{12}	C_{44}	K_S	C'_{11}	C'_{12}	C'_{44}	K'_S	
MgO	2.974	0.958	1.562	1.628	8.70	1.42	1.09	3.85	*Spetzler* [1970]
	2.966	0.951	1.558	1.623	9.16	1.82	1.12	4.27	*Chang and Barsch* [1969]
	2.967	0.951	1.560	1.623	9.48	1.99	1.16	4.49	*Anderson and Andreatch* [1969]
Range (%)	0.2	0.5	0.3	0.3	8	30	7	10	
NaCl	.4956	.1303	.1280	.251	11.65	2.06	0.37	5.26	*Spetzler et al.* [1972]
	.4942	.1269	.1281	.249	11.62	1.58	0.10	4.93	*Drabble and Strathen* [1967]
	.4958	.1306	.1279	.252	11.89	2.13	0.37	5.38	*Swartz* [1967]
	.4899	.1257	.1272	.247	11.66	2.08	0.37	5.27	*Bartels and Schuele* [1965]
Range (%)	1	3	0.7	2	2.5	25	25	6	
TiO_2	2.701	1.766	1.239	2.10	6.29	9.02	1.08	6.9	*Fritz* [1974]
	2.714	1.780	1.244	2.15	6.47	9.10	1.10	6.8	*Manghnani* [1969]
Range (%)	0.5	0.2	0.4	2	3	1	2	1.5	
Mg_2SiO_4	3.284	0.639	0.652	1.28	8.47	4.67	2.12	5.36	*Kumazawa and Anderson* [1969]
	3.291	0.663	0.672	1.29	8.32	4.30	2.12	4.83	*Graham and Barsch* [1969]
Range (%)	0.2	4	3	1	2	9	0	10	

a. Not all of the single-crystal moduli are shown for TiO_2 (tetragonal) and Mg_2SiO_4 (orthorhombic).

II. EXPERIMENTAL METHODS

The ultrasonic system, illustrated schematically in Figure 1, is described in detail elsewhere [*O'Connell et al.*, in preparation] and is based on the phase comparison technique [*McSkimin*, 1950].

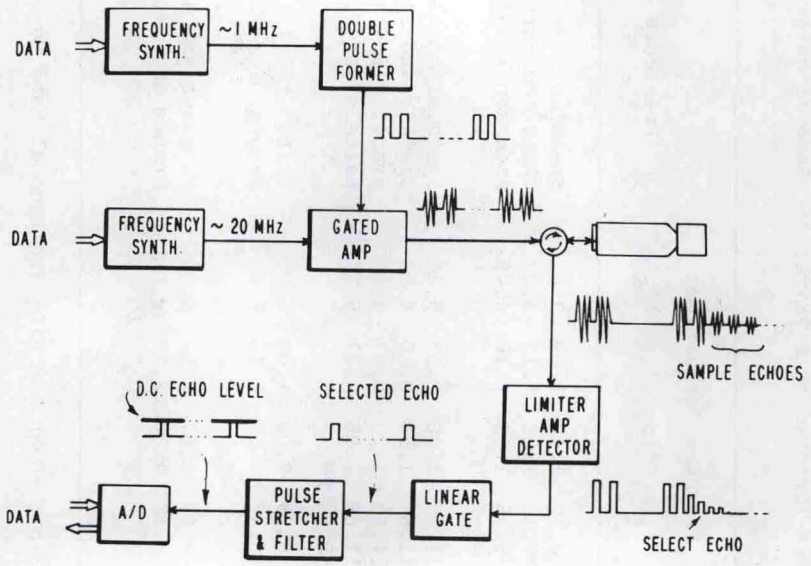

Fig. 1. Schematic diagram of the ultrasonic interferometer. Lines marked DATA indicate connection to minicomputer.

The instrumentation is similar to that described by *Spetzler* [1970]. An RF (carrier) wavetrain is gated to produce two RF pulses, which are phase coherent--i.e., the phase relationship of the pulses is the same as in the original wavetrain, independent of the spacing of the pulses. The electrical pulses are converted to acoustic pulses in the sample via a quartz transducer and the spacing of the pulses is adjusted so that the second pulse is superimposed on an echo of the first pulse in the sample. Alternate constructive and destructive interference of the pulses can be obtained by varying the carrier frequency. One echo from the train of echoes is selected with a linear gate, and its peak amplitude is converted to a DC output. The carrier frequency and pulse spacing are digitally controlled by an on-line minicomputer,

which also monitors echo amplitude. The computer is programmed to sweep through a specified range of carrier frequency and record the echo amplitude as a function of frequency, and it is also used to process the data as described below.

High pressures were generated with a Bridgman piston-cylinder apparatus with kerosene pressure medium. Pressure was determined to within 1% with a Heise gauge.

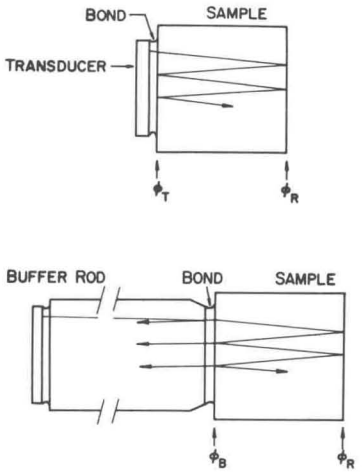

Fig. 2. Schematic diagram of the transducer-bond-sample and buffer rod-bond-sample assemblies in this study.

The transducer-buffer-bond-sample configurations used are illustrated in Figure 2. Samples used in this study--both about 1 cm in size--were a synthetic stoichiometric spinel ($MgAl_2O_4$) crystal obtained from Union Carbide and a synthetic MgF_2 crystal obtained from Optovac, Inc. Opposite faces on the samples were polished flat and parallel to within about one μ. A fused quartz buffer rod was used. Transducers were bonded by Dow Corning resin 276-V9 or, for some zero-pressure runs, phenyl salicylate. Coupling between the buffer rod and samples was achieved in several different ways: with dry lapped contact; with lapped contact immersed in a fluid pressure medium, such as isopentane; with a lapped contact wetted with the fluid (but not immersed); and with a V9 resin bond.

III. DATA PROCESSING

An example of amplitude-frequency data is illustrated in Figure 3(a). The broad amplitude envelope results from the combined response of the electronics and the transducer resonance (in this case the fundamental resonance frequency of the transducer

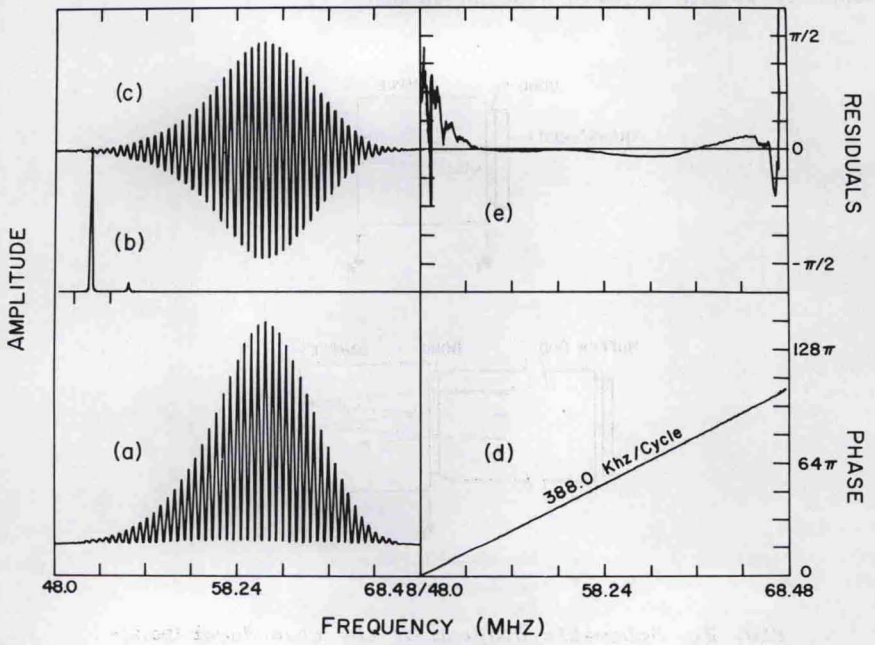

Fig. 3. (a) Amplitude-frequency interference pattern obtained from the ultrasonic interferometer. (b) Spectrum of a. Filter window is indicated by tick marks below spectrum. (c) Filtered amplitude-frequency data with envelope, harmonics, and noise removed. (d) Instantaneous phase of c versus frequency. (e) Residuals of d from a bestfit line.

was 20 Mhz). The narrow peaks result from successive constructive interferences of the superposed echoes in the sample. The condition for constructive interference is that the phase difference between successive echoes be equal to $2n\pi$, where n is an integer, i.e.:

$$\frac{4\pi fL}{v} + \phi_r = 2n\pi \qquad (1)$$

where f is the carrier frequency, L is the sample length, v is the sound velocity in the sample, and ϕ_r is the total phase shift produced by reflections at the sample faces. If the carrier frequency

is increased until the next constructive interference is achieved, the change in frequency, Δf, is given by

$$\frac{4\pi L}{v}\Delta f + \Delta\phi_r = 2\pi \qquad (2)$$

where $\Delta\phi_r$ is the accompanying change in ϕ_r. Thus, if $\Delta\phi_r$ is known or can be neglected, the velocity, v, can be determined by measuring Δf; Δf can be determined by directly measuring the frequencies at successive peaks and troughs [*Spetzler*, 1970], but their positions may be affected by the amplitude envelope and by noise. Instead, the phase of the sinusoid in Figure 3(a) was calculated continuously as a function of carrier frequency [*O'Connell et al.*, in preparation]. The phase of this sinusoid is directly related to the phase difference between superposed echoes in the sample; thus pressure derivatives can also be determined by measuring the phase as a function of pressure.

The first step in calculating the phase is to filter out the amplitude envelope and any harmonics and noise from the data. This is done via the spectrum (Figure 3b) of the data calculated by the Fast Fourier Transform (FFT) algorithm, and the result is illustrated in Figure 3(c). The filtered data are phase shifted by 90°, via a Hilbert transform in the frequency domain, and the "instantaneous" phase is then given by the inverse tangent of the ratio of the transformed to the original filtered data. The process is described in more detail by *O'Connell et al.* [in preparation]. The calculated variation of phase with carrier frequency is illustrated in Figure 3(d), and residuals from a best-fit straight line are shown in Figure 3(e). If reflection phase shifts in the sample could be neglected, the slope of this line would be a measure of the sound velocity in the sample. Small systematic deviations from linearity can be seen in Figure 3(e), which are interpreted below as arising from reflection phase shifts in the sample.

IV. TRANSDUCER-BOND PHASE SHIFTS

A sound wave reflected from a sample face to which a transducer is bonded is actually the superposition of waves reflected from three faces: the sample-bond and bond-transducer interfaces and the outer face of the transducer. The phase and amplitude of the resultant wave depend in a complicated way on the thickness and relative acoustic properties of the bond, transducer, and sample. This dependence, for the case of plane, parallel waves and interfaces, has been given by *Redwood and Lamb* [1956], who used the analogous theory of transmission lines [see also *McSkimin*, 1957; *Williams and Lamb*, 1958]; identical results can be obtained by considering plane elastic waves directly. The total transducer phase shift is

$$\phi_{tf} = 2\psi_{tf} - \pi \tag{3}$$

where

$$\tan \psi_{tf} = \frac{Z_f}{Z_s} \frac{Z_t \tan \theta_t + Z_f \tan \theta_f}{Z_f - Z_t \tan \theta_t \tan \theta_f} \tag{4a}$$

$$= \frac{Z_f}{Z_s} \tan (\eta_t + \theta_f) \tag{4b}$$

and

$$\tan \eta_t = \frac{Z_t}{Z_f} \tan \theta_t \tag{5}$$

Here, Z_s, Z_t, and Z_f are the acoustic impedance of the sample transducer, and bond ("film"), respectively, and θ is the thickness, in terms of the phase of the sound wave, of the transducer or bond

$$\theta = kl = 2\pi l/\lambda = 2\pi lf/v \tag{6}$$

where k is the wave number, λ is the wavelength, and l is the thickness. Subscript t or f in (6) would indicate transducer or bond properties, respectively. The acoustic impedance, Z, of a medium is the product of the density, ρ, and sound velocity, v, of the medium

$$Z = \rho v \tag{7}$$

The total reflection phase shift, θ_r, between successive echoes in the sample is the sum of (3) and a phase shift of π occurring on reflection at the other end of the sample. An example of calculated phase shifts as a function of carrier frequency is illustrated in Figure 4 for the case of a 10 Mhz quartz *P*-transducer (X-cut) bonded to a (100) face of MgF_2. The relevant acoustical properties are listed in Table 2, along with those of other materials discussed in this paper. Different bond thicknesses are represented by the parameter

$$\tau_f = \frac{l_f}{v_f} \tag{8}$$

which is the transit time (in nsec) of the wave through the bond. Wave velocities in typical bond materials are 1 to 2 km/sec. For v_f = 1 km/sec, τ_f is the bond thickness in μ.

For zero bond thickness, the phase shift is symmetrical about multiples of the transducer resonance frequency (in this case, the third), and equation (4) simplifies to

TABLE 2. Densities, Velocities, and Acoustic Impedances of Various Materials

Material	ρ, g/cm^3	v_p, km/s	v_s, km/s	Z_p	Z_s	Reference
α-quartz	2.65	5.75[a]	3.92[b]	15.2	10.3	*McSkimin et al.* [1965]
MgF_2 [100]	3.18	6.70	4.22	21.3	13.4	*Davies* [in preparation]
Fused quartz	2.20	5.9	3.8	13.0	8.4	*Peselnick et al.* [1967]
Spinel [100]	3.58	8.87	6.57	31.8	23.5	*Chang and Barsch* [1973]
276-V9 resin (20°C) (Dow-Corning)	-	-	-	2.2	1.0	*McSkimin and Andreatch* [1962]

a. For [100] (X-cut).

b. For [010] (Y-cut).

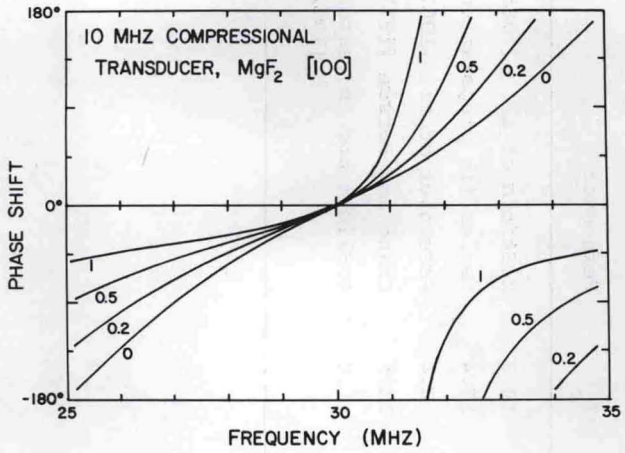

Fig. 4. Calculated transducer-bond phase shifts for compressional [100] waves in MgF_2 with a 10-Mhz quartz transducer bonded to the sample with V9 resin. Curves are labelled with bond transit time τ_f (nsec). Note that +180° is equivalent to -180° so that the curves in the lower right are continuations of the curves intersecting the upper margin.

$$\tan \psi_t = \frac{Z_t}{Z_s} \tan \theta_t. \qquad (9)$$

For non-zero bond thickness, the calculated phase shift is not symmetrical. At multiples of the transducer resonance frequency, the effect of the bond is very small, as pointed out by *McSkimin* [1961], but the bond effect can increase quite rapidly away from resonance multiples, especially on the high-frequency side (Figure 4).

Figure 5 compares some measured and calculated phase shifts as functions of carrier frequency. A reference measurement was made using a fused quartz buffer rod bonded to the sample. As described in the next section, the slope of this phase line should be very little affected by the buffer-sample bond. Accordingly, Figure 5 also shows the measured phase residual, with transducer bonded to sample, relative to a line with a slope measured with the buffer rod and coinciding with the measurement of 30 Mhz. The measured residual is compared with calculated transducer-bond phase shifts with τ_f = 0, 0.1, and 0.2 nsec. The form of the measured residual agrees well with that of the calculated phase shifts, and a value of τ_f between 0.1 and 0.2 nsec can be inferred from Figure 5. This corresponds to a bond thickness of the order of 0.2 to 0.4 μ, which is perhaps thinner than might have been

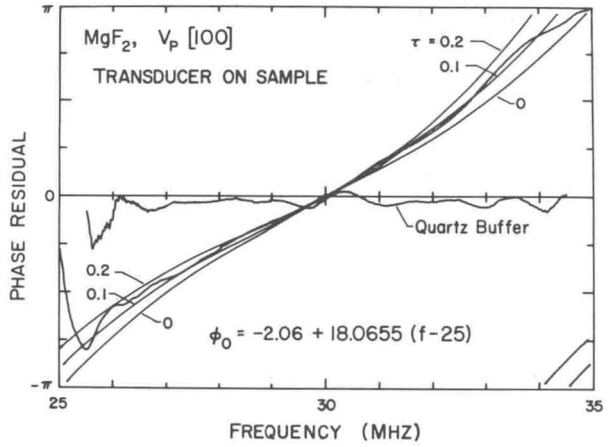

Fig. 5. Comparison of measured transducer-bond phase residuals (relative to phase obtained with buffer rod) with calculated phase shifts assuming τ_f = 0, 0.1, and 0.2 nsec.

expected. *McSkimin* [1961] reports θ_f = 5 to 15°, which, at 20 Mhz, corresponds to about τ_f = 0.7 to 2 nsec.

V. PRESSURE EFFECTS ON TRANSDUCER-BOND PHASE SHIFTS

Pressure affects, of course, all three components of the mechanical system: sample, bond, and transducer, but it is desired to isolate the effect on the sample from the effects on the other two. The effect of pressure on the transducer was considered by *McSkimin and Andreatch* [1962] who noted that the resonance frequency would change. The pressure derivatives of the resonance frequencies of X- and Y-cut quartz transducers (Table 3) were determined by *McSkimin and Andreatch* [1962] and *McSkimin et al.* [1965]. The effect of pressure on the bond was not discussed in detail by *McSkimin and Andreatch* [1962], their point being to establish that the bond phase shift is very small at the transducer resonance frequency and that it should change very little with pressure, providing the resonance frequency is followed. The effect of pressure on the bond phase shift will be discussed in more detail here, since it appears that the latter condition has not been strictly adhered to by many workers (including *McSkimin and Andreatch* [1962]). (*McSkimin and Andreatch* [1962] actually argued that the bond phase shift depends only on the total mass per unit area of the bond, and that the latter would not change with pressure. However, this conclusion depends on the assumption

TABLE 3. Transducer (α-quartz) and Bond Properties and Their Pressure Derivatives

Parameter	α-quartz[a]	Bond[b]
ρ, g/cm^3	2.65	1.0
K, Mbar	0.38	0.02
$\partial K/\partial P$	6.4	5.0
$M_p = \rho v_p^2$, Mbar	0.868	0.033
$\partial M_p/\partial P$	3.28	7.7
$M_s = \rho v_s^2$, Mbar	0.399	0.010
$\partial M_s/\partial P$	-2.69	2.0
$(\partial \ln f_r/\partial P)_p$, Mbar^{-1}	1.51	-
$(\partial \ln f_r/\partial P)_s$, Mbar^{-1}	-3.68	-

a. *McSkimin et al.* [1965].
b. Assumed.

that the bond compresses uniaxially, which is unlikely to be true, since it would require a large shear strength of the bond. Even with the assumption that the bond compresses isotropically, the phase shift changes very little with pressure, because it is so small to begin with, so that their main conclusion is still justified.)

A. Transducer Phase Shifts

A fairly common procedure has been to hold the carrier frequency constant at the zero-pressure resonance frequency, since the transducer resonance frequency varies by only a few percent over a pressure range of 10 kbar [e.g., *McSkimin et al.*, 1965]. A correction can be applied to allow for the changing transducer resonance frequency, and it is usually assumed that the bond effect remains negligible. Close to a transducer resonance frequency, where θ_t is close to an integral multiple of π, and for a vanishingly thin bond (negligible θ_f), equations (3) and (9)

yield approximately, and to within an additive factor of 2π,

$$\phi_t = 2\pi \frac{Z_t}{Z_s} \left(\frac{f}{f_r} - \frac{f}{f_{ro}}\right) \tag{10}$$

where f_{ro} is the value of f_r at zero pressure. Differentiating (10), and evaluating the result at zero pressure gives

$$\frac{\partial \phi_t}{\partial P} = -2\pi \frac{Z_t}{Z_s} \frac{f}{f_{ro}} \frac{\partial \ln f_r}{\partial P} \tag{11}$$

(Although Z_t and Z_s vary with pressure, they produce only a second-order effect.) A convenient expression can be derived for the corresponding correction to the derivative of the appropriate combination of elastic moduli, $M = \rho v^2$. The desired phase derivative is

$$\frac{\partial \phi_s}{\partial P} = \frac{\partial \phi_m}{\partial P} - \frac{\partial \phi_t}{\partial P} \tag{12}$$

where ϕ_m is the measured phase. The sample phase is $\phi_s = 4\pi fL/v$, so that

$$\frac{1}{\phi_s} \frac{\partial \phi_s}{\partial P} = -\frac{1}{2K} \left[\frac{K}{M} \frac{\partial M}{\partial P} - (1 - 2K\beta)\right] \tag{13}$$

where $\beta = -\partial \ln L/\partial P$ is the linear compressibility of the sample. The correction is, using (12),

$$\left[\frac{\partial M}{\partial P}\right]_{\text{corr.}} = -\frac{M v}{2\pi f L} \left(\frac{\partial \phi_t}{\partial P}\right). \tag{14}$$

Now combining (14) with (11)

$$\left[\frac{\partial M}{\partial P}\right]_{\text{corr.}} = \frac{v^2}{L} \left(\frac{Z_t}{f_r} \frac{\partial \ln f_r}{\partial P}\right). \tag{15}$$

Thus, apart from the transducer properties, the correction to $\partial M/\partial P$ depends only on the sample velocity and length. Some representative values are given in Table 4, for quartz transducers on MgF_2 and spinel. The corrections to the pressure derivatives of the moduli are of the order of 0.1 for compressional waves and -0.05 for shear waves.

TABLE 4. Representative Corrections to Pressure Derivatives of Elastic Moduli Due to Transducer Phase Shifts

Mode	v,km/s	L,mm	f_r, Mhz	$(\frac{\partial M}{\partial P})_{corr.}$	$\frac{\partial M}{\partial P}$
MgF_2[a]					
[001]P	8.01	10.80	20	.069	5.66
[110]P	8.15	10.80	10	.141	8.43
[001]S	4.22	9.64	20	-.035	0.79
[110]S[c]	2.82	10.80	20	-.014	-0.68
$MgAl_2O_4$[b]					
[001]P	8.88	10[d]	20	.091	5.15
[110]P	10.22	10	20	.120	5.85
[001]S	6.57	10	20	-.082	0.89
[110]S[c]	4.23	10	20	-.034	0.19

a. *Davies* [in preparation].

b. *Chang and Barsch* [1973].

c. Polarization $[1\bar{1}0]$.

d. Assume lengths for spinel.

Note that this difference in sign (arising from the opposite signs of the derivatives of the relevant quartz transducer frequencies [Table 3]). causes the corrections for some derived moduli to be compounded. This is most easily seen for an isometric material. If C_s denotes the modulus for a shear wave in the [110] direction, polarized in the $[1\bar{1}0]$ direction, then the bulk modulus is $K = C_{11} - 4C_s/3$, and $C_{12} = C_{11} - 2C_s$. The effect is illustrated in Table 5 for spinel (isometric) and MgF_2 (tetragonal).

TABLE 5. Corrections to Measured and Derived Modulus Derivatives Due to Transducer Phase Shifts, Illustrating the Compounding of Corrections in Derived Quantities

	Modulus, M.	$(\frac{\partial M}{\partial P})_{corr.}$	$\frac{\partial M}{\partial P}$
MgF_2	C_{11}	.10	5.01
	C_{33}	.07	5.66
	C_{12}	.15	6.37
	C_{13}	.24	4.18
	C_{44}	-.03	0.79
	C_{66}	.03	2.90
	K_S^a	.17	5.05
	μ^a	-.03	0.55
$MgAl_2O_4$	C_{11}	.09	5.15
	C_{12}	.16	4.76
	C_{44}	-.08	0.89
	K_S	.14	4.89

a. Isotropic aggregate modulus calculated from the Hashin-Shtrikman bounds [*Davies*, in preparation].

B. Bond Phase Shifts

Pressure affects the bond phase shift in two ways: directly, by changing the thickness and wave velocity of the bond material, and indirectly, if the carrier frequency is not continuously matched to the transducer resonance frequency to keep the bond phase shift minimal.

The pressure dependence of the properties of bond materials are not well known. For the purpose of assessing the importance of the effect, some representative properties have been assumed. These are shown in Table 3, and the resultant variations in density, velocities, and impedances to 40 kbar are given in Table 6. The variation in density was calculated from the Murnaghan equation

TABLE 6. Density, Velocities, and Impedances of a Hypothetical Bond Material as a Function of Pressure[a]

P,kbar	ρ,g/cm^3	v_p,km/s	v_s,km/s	Z_p	Z_s
0	1.00	1.82	1.00	1.82	1.00
10	1.28	2.92	1.53	3.75	1.96
20	1.43	3.61	1.87	5.16	2.67
30	1.53	4.14	2.14	6.35	3.28
40	1.62	4.59	2.36	7.41	3.81

a. Assumed bond properties are given in Table 3.

$$\rho = \rho_0 \left(1 + \frac{K'}{K} P\right)^{1/K'} \tag{16}$$

(where $K' = \partial K/\partial P$), which is derived from the assumption that the bulk modulus varies linearly with pressure. Consistent with this, the longitudinal and shear moduli were also assumed to vary linearly with pressure. The bond was assumed to compress isotropically, so that ℓ is proportional to $\rho^{-1/3}$. The velocities and impedances increase by factors of 2 to 4 in this pressure range, and θ_f (equation 6) decreases by a comparable amount, especially in the first few kbars. The effect of changing thickness on θ_f is relatively minor. This rapid effective thinning of the bond (relative to the sound wavelength in the bond) is important because it means that even if the frequency deviates from the transducer resonance frequency at high pressures, the bond phase shift may still not be large.

The total transducer-bond phase shift, including the indirect effect on the bond phase shift due to the variation of transducer resonance frequency (assuming fixed carrier frequency), has been calculated from equations (3-5), assuming bond properties similar to those in Table 6 and neglecting the variation of sample and transducer impedances. Results for a 10 Mhz quartz transducer on a [100] MgF_2 sample (see Tables 2 and 3) are illustrated in Figures 6 and 7 for fixed carrier frequencies f = 29, 30, and 31 Mhz. For $\theta_f = 0$, the variation of phase shift with pressure arises from the variation of the transducer resonance frequency. At f = 30 Mhz, the additional bond phase shift is fairly small at all pressures. The curves for f = 29 and 31 Mhz are included to illustrate more clearly the effects of pressure on bond phase

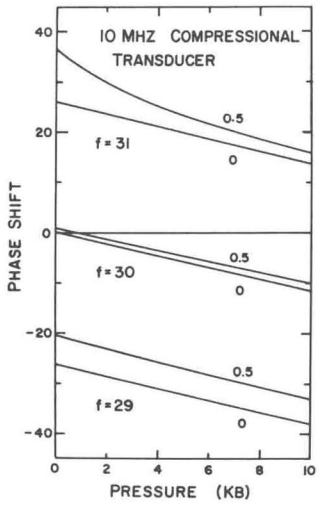

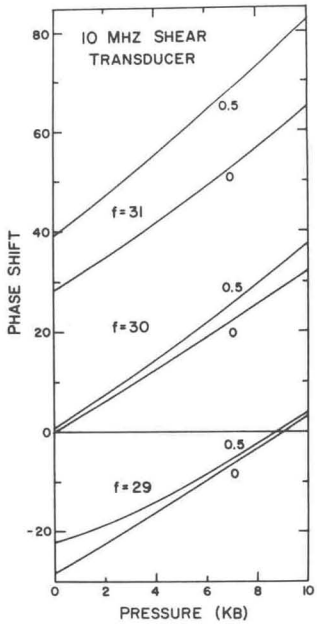

Fig. 6. (Left) Estimated effect of pressure on transducer-bond phase shifts for compressional [100] waves in MgF_2 with a 10-Mhz quartz transducer. Curves are for τ_f = 0 and 0.5 nsec and carrier frequency f = 29, 30, and 31 Mhz. Bond properties are estimated (Table 3). Fig. 7. (Right) As in Figure 6 for shear waves.

shifts. In Figure 6, at f = 31 Mhz, the bond phase shift decreases rapidly with increasing pressure, both because of the decreasing effective thickness of the bond and because f_r increases toward f. On the other hand, at f = 29 Mhz, f_r increases away from f, and the effects roughly cancel, so that the bond phase shift is fairly constant. These situations are reversed in Figure 7 because f_r decreases with increasing pressure for shear waves.

The reality of these effects was tested by comparison with some measurements on MgF_2 [100] compressional waves. Measurements of phase versus f at pressures up to 7 kbar were converted to phase versus pressure at frequencies f = 30, 31, and 32 Mhz. The results are shown in Figure 8(a). A systematic difference in slopes at the different frequencies, amounting to about 5%, can be discerned. Residuals relative to a line through the 30 Mhz data

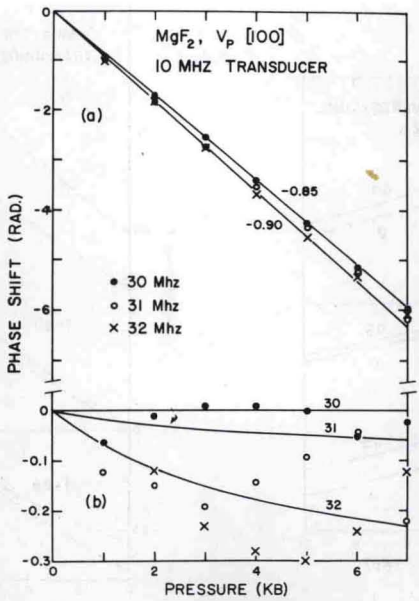

Fig. 8. (a) Measured phase shifts versus pressure (normalized to 30 Mhz) at 30, 31, and 32 Mhz for compressional [100] waves in MgF_2. Lines are labelled with slopes (rad/kbar). (b) Residuals of measured phase shifts relative to line through 30 Mhz data, compared with calculated transducer bond phase shifts, assuming bond properties (Table 3) and $\tau_f = 0.2$ nsec.

(shown in Figure 8(b)) are compared to calculated transducer-bond phase shifts, assuming $\tau_f = 0.2$ nsec (see previous section). Although there is considerable scatter in the residuals, their ordering and magnitudes are quite comparable to the calculated phase shifts, which is evidence that the phase shifts are being correctly described and that there are no other important effects on the measurements.

If the carrier frequency is accurately fixed at the transducer resonance frequency, the effect of the bond phase shift should be quite small. For instance, in Figure 7 the effect of the bond at 30 Mhz is about 15% of the effect of the transducer on the slope. Since the latter changes the value of $\partial M/\partial P$ by about -0.05, the effect of the bond phase shift on $\partial M/\partial P$ would be less than -0.01. If f deviates from f_{ro}, then of course the bond effect can be considerably larger. For instance, in Figure 6, at 31 Mhz the bond effect is comparable to that of the transducer.

Measurements of second pressure derivatives of elastic moduli

have been reported by several workers [e.g., *Chang and Barsch*, 1967, 1973; *Frisillo and Barsch*, 1972]. Bond phase shifts could be significant sources of error in such measurements. Some curvature is evident in Figures 6 and 7, even for f = 30 Mhz. In Figure 7 at f = 30 Mhz, the slope increases by about 20% over the 10 kbar pressure range. This would correspond to a change in $M' = \partial M/\partial P$ of about -0.01. Assuming a bulk modulus K = 2 Mbar then gives a change in KM'' of about -2. This is comparable to the accuracy claimed in some of the measurements referred to above. Of course, any deviation of f from f_{ro} could considerably increase this effect.

C. Other Measurement Procedures

Spetzler [1970] determined pressure derivatives by measuring the pressure dependence of the peaks and troughs in the interference pattern (Figure 3a), i.e. by measuring the derivative $(\partial f/\partial P)_\phi$ rather than $(\partial \phi/\partial P)_f$. (*Spetzler* used a buffer rod, but the same procedure might be used without a buffer rod.) The transducer-bond phase shifts in this case will depend on the difference between the transducer and sample derivatives, $\partial(f_s - f_r)/\partial P$. The expressions above can be generalized to allow for the variation of the carrier frequency f. For compressional waves, both derivatives will be positive and will tend to cancel, so that the bond phase shifts should be no greater than when f is constant. For shear waves, however, the sample derivative will most commonly be positive, while the transducer derivative is negative (for quartz), so that f_s may deviate considerably from f_r and the bond phase shift become significant. Also, *Spetzler* [1970] averaged measurements on a series of peaks and troughs near the transducer resonance frequency. If this was done without a buffer rod, significant bond phase shifts might affect those peaks and troughs not initially close to the transducer resonance frequency.

Another procedure that might be followed is to use the maximum amplitude response of the transducer to attempt to follow the resonance frequency of the transducer under pressure. However, when a transducer is bonded to a sample, the frequency at which maximum amplitude is obtained is not the free resonance frequency of the transducer, owing to the effect of the bond between the transducer and the sample. The expression for the response of the bonded transducer can be found in *Mason* [1958].

Figure 9 shows the relative amplitudes calculated for an X-cut quartz transducer bonded with V9 resin to a sample of olivine; curves are shown for several bond thicknesses ranging from 0 to 2 μm. The shift of the point of maximum amplitude to higher frequencies, owing to the presence of the bond, is apparent. The variation of the point of maximum amplitude with pressure is shown in Figure 10. The pressure dependence arises primarily from the change of the properties of the bond with pressure.

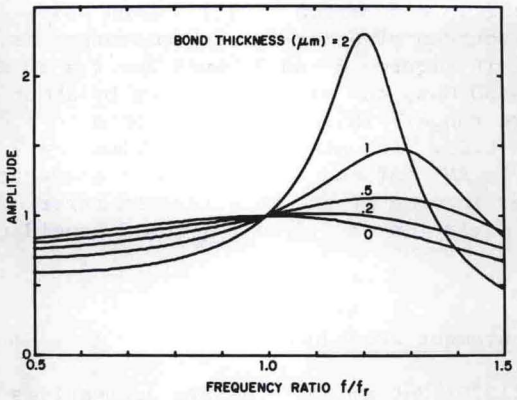

Fig. 9. Calculated relative amplitude versus frequency of X-cut quartz transducer bonded to olivine with various thicknesses of V9 resin.

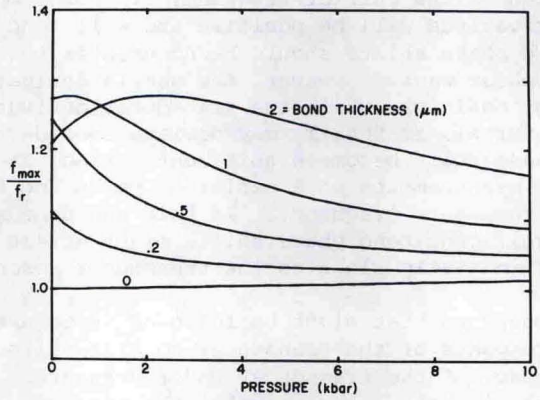

Fig. 10. Calculated frequencies of maximum amplitude in Figure 9 as a function of pressure.

If during an experiment the point of maximum amplitude was (wrongly) taken to be the resonant frequency of the transducer, then substantial errors could occur. It can be seen in Figure 4 that the phase shift due to the bond can be quite large, 1 or 2 Mhz above the free resonance frequency. Figure 11 shows the bond phase shift as a function of pressure when the operating frequency is kept at the point of maximum amplitude as shown in Figure 10. The phase shifts can easily be a large fraction of π, and vary significantly with pressure. A rough calculation shows that the

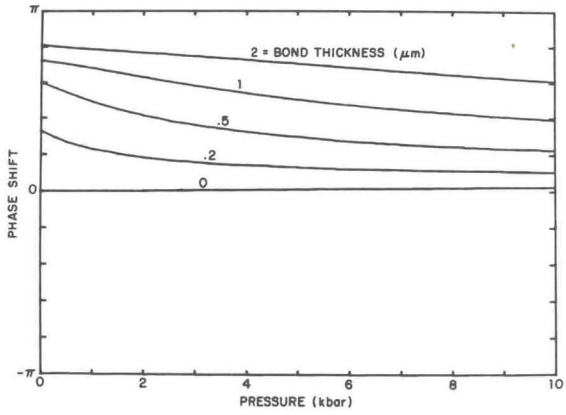

Fig. 11. Calculated transducer-bond phase shift versus pressure for the case where the operating frequency is kept at the frequencies of maximum amplitude of Figure 10.

magnitude of the phase shifts could cause errors of the order of ½% in determining absolute velocities, and errors of several tens of percent in pressure derivatives of velocities for typical minerals.

These potential errors are large, and would be best avoided. This is easily done by operating the transducer at its free resonant frequency in experiments using the pulse superposition technique. It is not clear from published reports of experiments if this procedure has been always used in pulse superposition measurements, but in at least some experiments the transducer has been operated at the maximum amplitude frequency rather than at the free resonance frequency [*E. Schreiber*, personal communication].

VI. BUFFER ROD-BOND PHASE SHIFTS

The phase shift which occurs upon reflection in the sample at a buffer rod-sample interface (Figure 2) is [*McSkimin*, 1950; 1957]

$$\phi_r^- = \tan^{-1} \frac{2Z_f Z_s (Z_b^2 - Z_f^2) \tan\theta_f}{Z_f^2 (Z_b^2 - Z_s^2) + (Z_f^4 - Z_s^2 Z_b^2) \tan^2\theta_f} \quad (17)$$

where subscript b denotes buffer rod properties, and superscript "-" denotes the reflection of a wave traveling in the negative (leftward) direction (Figure 2). This phase shift (plus the phase shift of π occurring at the free end of the sample) applies to superpositions of all but the first and second reflections received by the transducer. Since the first reflection is from the buffer side of the interface, and the wave does not penetrate the sample, whereas the second and succeeding reflections are

transmitted twice through the interface, the appropriate phase difference due to the interface is

$$\phi_1 = 2\phi_t - \phi^+_r \tag{18}$$

where ϕ_t, the phase shift on transmission, is

$$\phi_t = \tan^{-1} \frac{Z_s Z_b + Z_f^2}{Z_f (Z_s + Z_b)} \tan \theta_f \tag{19}$$

and ϕ^+_r has the same form as (17), but with Z_b and Z_s interchanged. The superposition of the first and second reflections will be referred to as echo 1, and succeeding combinations as echoes 2, 3, and so on.

An example of calculated buffer-bond phase shifts is shown in Figure 12 for the case of shear waves in the [100] direction in spinel, with a fused quartz buffer rod and a V9 bond. The

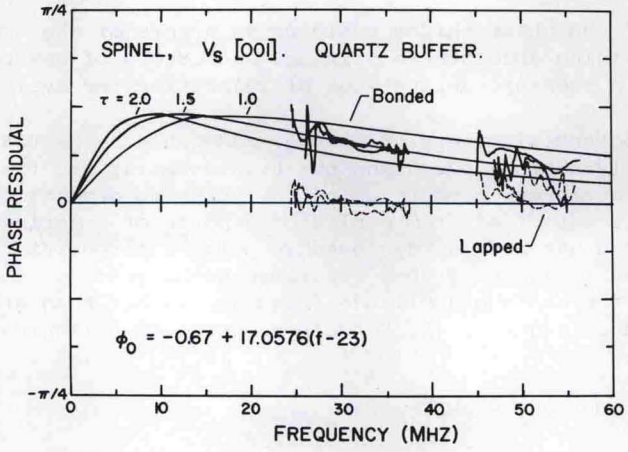

Fig. 12. Measured phase residuals (solid traces) relative to phase with dry lapped buffer-sample contact (dashed traces) for shear [100] waves in spinel, with fused quartz buffer rod bonded to sample, compared with calculated buffer-bond phase shifts (solid curves) for τ_f *= 1.0, 1.5, and 2.0 nsec.*

relevant properties are given in Table 2. Curves are shown for three different values of τ_f. It can be seen that the effect of thinning the bond is to increase the frequency at which the maximum phase shift occurs. Compared to these in Figure 12 are some measured phase residuals in two frequency intervals (around the third and fifth harmonics of a 10 Mhz transducer). Measurements with a dry lapped contact between the buffer and sample (i.e., no

bond) were taken as the standard, and the other measurements referred to a best-fit line through these. Another series of measurements was made with a V9 bond between the buffer and the sample. All runs were duplicated. It can be seen in Figure 12 that the results are consistent with a bond having a value of τ_f between 1 and 2 nsec. For the wave velocity of 1 km/sec measured for V9 (Table 2), this corresponds to a bond thickness between 1 and 2 μ. These results indicate that the phase shift due to the bond has been resolved and that it is described by equation (17) derived from plane wave theory.

Results of similar measurements with compressional waves are not so easily interpreted, however. Figures 13 and 14 compare calculated phase shifts with measured residuals for the cases of

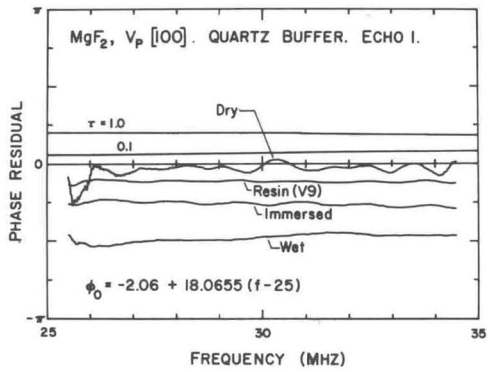

Fig. 13. As in Figure 12, for echo 1 of compressional [100] waves in MgF_2, τ_f = 0.1 and 1.0 nsec, and various buffer-sample contacts (see text).

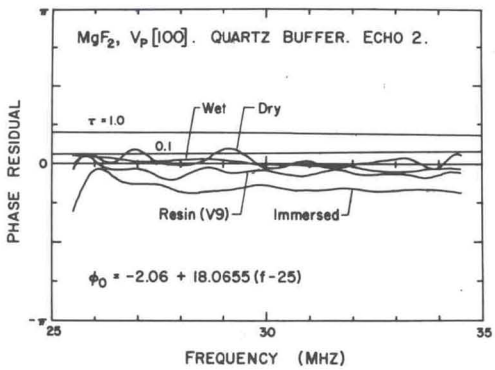

Fig. 14. As in Figure 13, for echo 2.

[100] compressional waves in MgF_2, echoes 1 and 2, with a fused quartz buffer rod. The measurements with the dry lapped contact have again been taken as references for the calculation of residuals. It can be seen that the measured effect of the V9 bond relative to the dry lapped contact is smaller and of opposite sign than expected.

Measurements were made in two other situations. First, in an attempt to get a very thin bond, a dry lapped contact was first achieved and the contact was then squirted with isopentane (used in other experiments as a pressure medium). The result was an immediate enhancement of the signal, indicating that the liquid quickly penetrated the contact. Although isopentane is quite volatile, the enhancement would persist for some time (5 to 15 min) before the signal would drop to its original level relatively rapidly (the order of one minute), indicating that the isopentane had evaporated. The phase shift measured for this "wet" contact was very small for echo 2, but about 90° for echo 1 (Figures 14 and 13)! To test for the possibility that the above procedure had not completely wetted the contact, a dry lapped contact was again established, and the part of the assembly (the sample and part of the buffer rod) was immersed in isopentane. The resulting phase shifts are different again (Figures 13 and 14): they are more negative than with the V9 bond for both echoes 1 and 2. This suggests that the previous procedure had indeed only partially wet the interface.

The explanation for these results is not clear at this stage, but one interpretation will be suggested below. There is an indication that the assumptions of simple plane wave theory may not be appropriate. The maximum calculated phase shift (see Figure 12) is controlled by the impedance ratio of the buffer and sample, Z_b/Z_s (at least, when Z_b is less than Z_s; when Z_b is greater than Z_s, the phase shift increases to π at zero frequency). It is about 40° in Figures 13 and 14 ($Z_b/Z_s = 0.61$) and about 20° in Figure 12 ($Z_b/Z_s = 0.36$). It approaches 90° only as Z_b/Z_s approaches 1.0. Thus, even if the wrong reference were used in calculating the residuals, or if their signs were wrong, the plane wave theory cannot explain the range of measured residuals of about 90° for echo 1 (Figure 13).

It may be seen in Figures 13 and 14 that the measured phase shifts with the V9 bond and the immersed contact are mutually consistent if it is assumed that the "dry lapped" measurements are not the correct reference (i.e., do not correspond to zero phase shift). The V9 bond and immersed results can be matched by the calculated curves by assuming τ_f is about 1 nsec for the V9 bond (comparable to the results found with shear waves, Figure 12) and about 0.1 nsec with the contact immersed in isopentane (consistent with the expectation of getting a much thinner bond in that case). The results for the wet and dry contacts then require some other explanation.

Even with accurately lapped surfaces, only partial contact between the buffer and the sample can be expected (considerable

manual force is required to achieve a measurable signal), and presumably this contact is at a series of points scattered across the surfaces. The area of contact would be expected to vary with the normal force across the interface. A passing shear wave would not affect this force, but a compressional wave would. Thus, parts of the surfaces may be in contact, and thus transmitting the stress wave, only near peaks in a compressional wave; further, that part of the wave might be phase delayed because of the time required to bring the surfaces into contact, which might be a considerable fraction of the period of the wave. It is not at all clear at this stage that this kind of mechanism can explain the observations, but it serves to illustrate the possibility that the mechanical coupling at lapped contacts may be complicated and nonlinear. Partial wetting of the interface might produce additional effects, such as "squirting" of the liquid during compressional cycles, which could considerably modify the coupling. Presumably, complete wetting with even a weak couplant, such as isopentane, could eliminate or considerably reduce these effects. On the other hand, even the "dry" contact might be affected by condensation of vapor or by surface films in the interface. Although the surfaces were carefully cleaned with solvent before assembly, no extraordinary precautions were taken to keep them clean and dry. (Some measurements were made under modest vacuum, about 0.01 atm, with no observable effect. We also had to contend with curious colleagues, who wondered if we intended extrapolating to mantle pressures from measurements at 0 and 1 atm.) Until a better understanding of these phenomena is achieved, it seems clear that the results of measurements with buffer rods should be treated with some caution, especially in view of the large phase shifts observed with the dry or "wet" contacts.

These cautionary remarks also apply to measurements of pressure derivatives. It is premature to try to estimate the effect of pressure on the lapped contacts, except to note that, unless they are remarkably unaffected, they could be significant sources of error.

Spetzler et al. [1972] reported a large negative second pressure derivative of the bulk modulus of NaCl, which it is difficult to reconcile with shock compression data to 250 kbar [*Fritz et al.*, 1971], as was discussed by *Spetzler et al.* [1972]. They used a buffer rod, in dry lapped contact with the sample, and a gas (Ar) pressure medium. The quality of the contact may have been somewhat better than in the present experiments because the surfaces were polished flat to within 1/10 wavelength of light, NaCl is relatively soft, the surfaces were very carefully wrung together, and the contact area was only 5 mm in diameter [*Spetzler et al.* 1969a, 1969b, 1972; *Spetzler*, personal communication]. However, their measured zero-pressure velocities differ significantly from the extrapolation of the higher-pressure velocities to zero pressure. This may indicate some problem with the zero-pressure contact which was reduced as the Ar acoustic impedance increased at higher pressures.

Assuming that a bonded contact between the buffer and sample is "well behaved," as suggested above, the effect of pressure on the bond phase shift can be estimated. Bond properties similar to those in Table 3 were again assumed. Some results are illustrated in Figure 15 for compressional [100] waves in MgF_2, a fused quartz buffer, and several carrier frequencies and bond thicknesses.

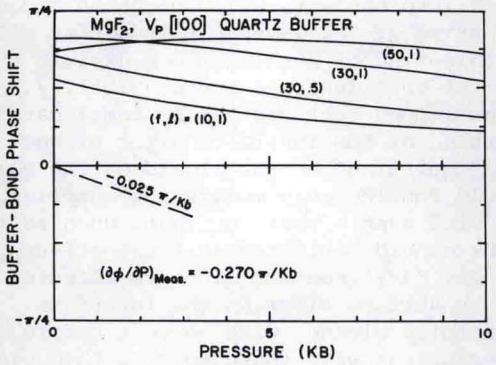

Fig. 15. Estimated effect of pressure on buffer-bond phase shifts for compressional [100] waves in MgF_2, fused quartz buffer rod, τ_f = 0.5 and 1 nsec and carrier frequency f = 10, 30, and 50 Mhz.

Again, the effective thickness of the bond decreases rapidly with increasing pressure. As mentioned earlier, this causes the position of the maximum phase shift to move to higher frequencies. Thus, in some cases, the phase shift first increases with increasing pressure, then decreases; in other cases, it decreases montonically. The magnitude of the effects are significant: for the curves in Figure 15, the slopes are up to 3° kbar. This could amount to 5% of the total phase shift; for the example in Figure 15, the measured phase shift was 49.2° kbar.

The buffer-bond phase shift can be reduced by having a thinner bond (as may be the case for the "immersed" contact discussed above), and by keeping the buffer to sample impedance ratio small. Values of Z_b/Z_s close to or greater than 1 allow phase shifts of up to 90°. (This may be another source of error in the measurements of *Spetzler et al.* [1972], since the relevant impedances of NaCl are probably all less than those of the fused quartz buffer rod used, although it is difficult to evaluate because of the uncertainty in the nature of the bonding.)

VII. CONCLUSIONS

No common source of errors in measurements of pressure

derivatives of elastic properties has been clearly identified in this study, but some possibilities may be suggested. Most measurements seem to have been done with the transducer bonded directly to the sample, and many of those measurements were done by the method described by *McSkimin* [1961] and *McSkimin and Andreatch* [1962]. If their procedure is closely followed, in particular, if the carrier frequency is fixed at the zero pressure (free) resonance frequency of the transducer and the correction made for the change of the resonance frequency with pressure, then the effect of the bond on the pressure derivatives of elastic moduli should amount to less than 0.02. If the transducer correction is neglected, an error of the order of 0.1 might be incurred in the modulus derivative. If, in any experimental procedure in which the transducer is bonded to the sample, the carrier frequency deviates more than a few percent from the transducer resonance frequency, then the bond phase shift might cause significant error, especially if the deviation is at zero pressure, where the bond effects are largest. Measurements reported here demonstrate an error of 5% in the slope (i.e., about 0.25 in the pressure derivative of modulus) incurred by operating a 10 Mhz transducer at 32 Mhz rather than 30 Mhz.

On the other hand, it seems that measurements made with buffer rods between transducers and samples may be subject to significant errors unless special precautions are taken. It has been estimated here that a conventional bond between the buffer and sample could change the measured modulus derivative by the order of 0.25, a very thin bond (such as was apparently achieved here by immersing a lapped contact in a liquid pressure medium) would produce a somewhat smaller effect, perhaps of the order of 0.05. The ratio of buffer to sample acoustic impedance should be significantly different from (preferably less than) unity, to reduce the bond phase shift.

It seems that the (not unreasonable) hope of *Spetzler et al.* [1969*a*,*b*; also, *Spetzler*, 1970; *Spetzler et al.*, 1972] of avoiding the bond (or interface) phase shift by using a dry lapped contact has not been completely borne out by the results reported here, at least for compressional waves. Dry lapped contact seems to produce substantial phase shifts in compressional waves. Since the mechanism producing the phase shift is not understood at present, its pressure dependence cannot be estimated, but it could easily produce substantial errors in measured pressure derivatives. With what is inferred to have been a partially wetted lapped contact, even larger phase shifts were observed at zero pressure. As indicated above, no anomalous buffer-sample interface phase shifts were observed for shear waves.

Further study, especially with buffer rods, should clarify these problems. In particular, a careful comparison at zero pressure (which was not achieved in the present study) of the relative phases measured with the transducer on the sample and with the various buffer rod-sample contacts should identify unambiguously which of the buffer-sample contacts are producing anomalous phase

shifts. Then, more measurements under pressure are required, both to confirm the expected effects of "normal" buffer-sample bonds and to determine the pressure dependence of the "anomalous" interface phase shifts.

Finally, we note again that the effects of transducer bonds can account for significant systematic errors, especially in the measurement of first and higher order pressure derivatives of elastic constants. The results of this paper show that such effects are in accord with theoretical predictions; consequently it is possible to correct for them. But in order to correct for such effects one must know the details of the experimental procedure, such as the operating frequency of the transducer. We strongly recommend that such details be routinely included in published reports, so that the effects of these and possibly other yet unknown systematic errors can be corrected for without repeating the experiment.

Acknowledgments. We are grateful to J. Peter Watt for assistance in computer program development, and to H. Spetzler for useful discussions. This research was supported by the Committee on Experimental Geology and Geophysics, Harvard University, and by National Science Foundation Grant GA38899 (Earth Sciences).

REFERENCES

Anderson, O. L., and P. Andreatch, Jr., Pressure derivatives of elastic constants of single-crystal MgO at 23° and -195.8°C, *J. Amer. Ceram. Soc., 49*, 404-409, 1966.

Bartels, R. A., and D. E. Schuele, Pressure derivatives of the elastic constants of NaCl and KCl at 295°K and 195°K, *J. Phys. Chem. Solids, 26*, 537-594, 1965.

Chang, Z. P., and G. R. Barsch, Non-linear pressure dependence of elastic constants and fourth-order elastic constants of cesium halides, *Phys. Rev. Lett., 19*, 1381-1383, 1967.

Chang, Z. P., and G. R. Barsch, Pressure dependence of the elastic constants of single-crystalline magnesium oxide, *J. Geophys. Res., 74*, 3291-3294, 1969.

Chang, Z. P., and G. R. Barsch, Pressure dependence of single-crystal constants and anharmonic properties of spinel, *J. Geophys. Res., 78*, 2418-2433, 1973.

Drabble, J. R., and R. E. B. Strathen, The third-order elastic constants of potassium chloride, sodium chloride, and lithium fluoride, *Proc. Phys. Soc., London, 92*, 1090-1095, 1967.

Frisillo, A. L., and G. R. Barsch, Measurement of single-crystal elastic constants of bronzite as a function of pressure and temperature, *J. Geophys. Res., 77*, 6360-6384, 1972.

Fritz, I. J., Pressure and temperature dependences of the elastic properties of rutile (TiO_2), *J. Phys. Chem. Solids, 35*, 817-826, 1974.

Fritz, J. N., S. P. Marsh, W. J. Carter, and R. G. McQueen, The Hugoniot equation of state of sodium chloride in the sodium chloride structure, in *Accurate Characterization of the High Pressure Environment*, edited by E. C. Lloyd, pp. 201-208, NBS Special Publication 326, Washington, D. C., 1971.

Graham, E. K., Jr., and G. R. Barsch, Elastic constants of single-crystal forsterite as a function of temperature and pressure, *J. Geophys. Res., 74*, 5949-5960, 1969.

Kumazawa, M., and O. L. Anderson, Elastic moduli, pressure derivatives, and temperature derivatives of single-crystal olivine and single-crystal forsterite, *J. Geophys. Res., 74*, 5961-5972, 1969.

Manghnani, M. H., Elastic constants of single-crystal rutile under pressure to 7.5 kilobars, *J. Geophys. Res., 74*, 4317-4328, 1969.

Mason, W. P., *Piezoelectric Crystals and Their Application to Ultrasonics*, Van Nostrand, Princeton, New Jersey, 1958.

McSkimin, H. J., Ultrasonic measurement techniques applicable to small solid specimens, *J. Acoust. Soc. Amer., 22*, 413-418, 1950.

McSkimin, H. J., Use of high frequency ultrasound for determining the elastic moduli of small specimens, *IRE Trans. on Ultrasonic Eng., PGUE-5*, 25, 1957.

McSkimin, H. J., Pulse superposition method for measuring ultrasonic wave velocities in solids, *J. Acoust. Soc. Amer., 33*, 12-16, 1961.

McSkimin, H. J., Variations on the ultrasonic pulse-superposition method for increasing the sensitivity of delay-time measurements, *J. Acoust. Soc. Amer., 37*, 864-871, 1965.

McSkimin, H. J., and P. Andreatch, Jr., Analysis of the pulse superposition method for measuring ultrasonic wave velocities as a function of temperature and pressure, *J. Acoust. Soc. Amer., 34*, 609-615, 1962.

McSkimin, H. J., P. Andreatch, Jr., and R. N. Thurston, Elastic moduli of quartz versus hydrostatic pressure at 25° and -195.8°C, *J. Appl. Phys., 36*, 1624-1632, 1965.

Peselnick, L., R. Meister, and W. H. Wilson, Pressure derivatives of elastic moduli of fused quartz to 10 kb, *J. Phys. Chem. Solids, 28*, 635-639, 1967.

Redwood, M., and J. Lamb, On the measurement of attenuation in ultrasonic delay lines, *Proc. Inst. Elec. Engrs., Pt. B., 103*, 773-780, 1956.

Spetzler, H., Equation of state of polycrystalline and single-crystal MgO to 8 kilobars and 800°K, *J. Geophys. Res., 75*, 2073-2087, 1970.

Spetzler, H., C. G. Sammis, and R. J. O'Connell, Equation of state of NaCl: ultrasonic measurements to 8 kbar and 800°C and static lattice theory, *J. Phys. Chem. Solids, 33*, 1727-1750, 1972.

Spetzler, H., E. Schreiber and D. Newbigging, Coupling of ultra-

sonic energy through lapped surfaces at high temperature and pressure, *J. Acoust. Soc. Amer.*, *45*, 1057-1058, 1969*a*.

Spetzler, H., E. Schreiber, and L. Peselnick, Coupling of ultrasonic energy through lapped surfaces: application to high temperatures, *J. Acoust. Soc. Amer.*, *45*, 520, 1969*b*.

Swartz, K. D., Anharmonicity of sodium chloride, *J. Acoust. Soc. Amer.*, *41*, 1083-1092, 1967.

Williams, J., and J. Lamb, On the measurement of ultrasonic velocity in solids, *J. Acoust. Soc. Amer.*, *30*, 308-313, 1958.